

1 **In-situ unsaturated zone water stable isotope (^2H and ^{18}O)**
2 **measurements in semi-arid environments: Potentials and**
3 **limitations.**

4

5 **M. Gaj^{1,2} M. Beyer¹, P. Koeniger¹, H. Wanke³, J. Hamutoko³, T. Himmelsbach¹**

6 [1]{Federal Institute for Geosciences and Natural Resources (BGR), Stilleweg 2, Hannover,
7 Germany}

8 [2]{Chair of Hydrology, Faculty of Environment and Natural Resources, University of
9 Freiburg, Fahnenbergplatz, 79098 Freiburg, Germany}

10 [3]{Department of Geology, University of Namibia, (UNAM) Windhoek, Namibia}

11

12 Correspondence to: Marcel Gaj (marcel.gaj@bgr.de)

13

14

1 **Abstract**

2 Stable isotopes (deuterium, ^2H , and oxygen-18, ^{18}O) of soil water were measured in the field
3 using liquid water isotope analyzer (tunable off-axis integrated cavity output spectroscope,
4 OA-ICOS, LGR) and commercially available soil gas probes (BGL-30, UMS, Munich) in the
5 semi-arid Cuvelai-Etosha Basin (CEB), Namibia.

6 Results support the applicability of an in-situ measurement system for the determination of
7 stable isotopes in soil pore water. High spatial and temporal resolution was achieved in the
8 study area with reasonable accuracy and measurements were in agreement with laboratory-
9 based cryogenic vacuum extraction and subsequent cavity ring down laser spectroscopic
10 isotope analysis (CRDS). After drift correction of the in-situ isotope data, precision for over
11 140 measurements taken during two consecutive field campaigns (June and November, 2014)
12 were 1.8 ‰ and 0.48 ‰ for $\delta^2\text{H}$ and $\delta^{18}\text{O}$, respectively. Mean accuracy using quality check
13 standards was 5 ‰ and 0.3 ‰ for $\delta^2\text{H}$ and $\delta^{18}\text{O}$, respectively. The isotope depth profiles are
14 used quantitatively to calculate a soil water balance. The contribution of transpiration to total
15 evapotranspiration ranged between 72 % and 92 %. Short after a rain event the contribution of
16 transpiration was much lower with 35 % to 50 %.

17 Potential limitations of such an in-situ system are related to environmental conditions which
18 could be extended using a temperature controlled chamber for the laser spectrometer. Further,
19 the applicability of the system using previously oven dried soil material might be limited by
20 physicochemical soil properties (i.e. clay minerals). Furthermore the influence of soil respired
21 CO_2 to isotope values within the root zone could not be deduced from the data.

22
23

1 1 Introduction

2 Water stable isotopes of water have been successfully used for decades as powerful proxies
3 for the description of water fluxes such as infiltration in humid (Saxena, 1987) or semi arid
4 regions (Dincer et al., 1974; Allison and Hughes, 1983), evapotranspiration (Barnes and
5 Allison, 1988, Wang et al., 2012; Dubbert et al., 2013; Skrzypek et al., 2015), plant root water
6 uptake (Dawson and Ehleringer, 1991; Ehleringer and Dawson, 1992; Dawson, 1996; Yang et
7 al., 2010), hydraulic redistribution (Dawson, 1993; Caldwell et al., 1998), and in catchment
8 hydrology (e.g., Sklash and Farvolden, 1979; Richard and Shoemaker, 1986; Tetzlaff et al.,
9 2007; Kendall and McDonnell, 2012). Soil water stable isotopes provide information on flow
10 paths way and mixing within the unsaturated zone (Gazis and Feng, 2004; Stumpp and
11 Maloszewski, 2010; Garvelmann et al., 2012; Mueller et al., 2014). Soil water stable isotope
12 studies were also used to reduce parameter uncertainty in unsaturated zone model approaches
13 (Sprenger et al., 2014). Further work has been done to use soil water stable isotopes for
14 quantitative recharge estimations which are actively discussed in early and recent reviews
15 (e.g., Allison et al., 1994; Scanlon et al., 2002). But the usefulness of evaporation profiles to
16 determine recharge rates remains debatable (Herczeg et al., 2011).

17 In most unsaturated zone studies manual removal of soil samples and a subsequent extraction
18 of soil water in the laboratory was necessary using either vacuum extraction (e.g., West et al.,
19 2006; Koeniger et al., 2011; Orlowski et al., 2013), equilibration (e.g., Wassenaar et al.,
20 2008), mechanical squeezing, azeotropic distillation or centrifugation methods (e.g., Walker et
21 al., 1994; Kelln et al., 2001). These methods cause both disturbance to the integrity of the
22 natural soil system and possible evaporation during the sampling procedure. The latter is
23 especially important for dry soils. Hence, soil water extraction techniques are labor intensive
24 and expensive which is limiting the use of stable isotopes compared to the other state
25 variables such as soil moisture or matrix potential measurements. Indeed, there are suction
26 cup installations which allow a removal of soil water non-destructively but they are not
27 applicable in (semi-) arid environments. This is especially true during the dry season where
28 vapor transport (i.e. evaporation) is the dominant driver for water fluxes in the unsaturated
29 zone but is much less studied than the liquid water component (Soderberg et al., 2012). In this
30 context, the determination of stable isotopes from sampling the vapor of the pore space
31 appears useful.

1 Principles to sample soil air for the determination of stable isotopes were already indicated by
2 Allison et al., (1987) and Schack-Kirchner et al., (1993). An attempt to measure stable
3 isotopes in a sandy loam using a liquid water analyzer (OA-ICOS, Los Gatos Research, DLT-
4 100) is presented in a recent review by Soderberg et al., (2012). The first study monitoring
5 stable isotopes in-situ in unsaturated sandy soil water under laboratory conditions made use of
6 poly-propylene (PP) membranes (Rothfuss et al., 2013). Measurements were performed with
7 a cavity-ring-down spectrometer (CRDS) (L1102-I, Picarro, CA, USA) calibrated with liquid
8 water injections using a vaporizer unit. Volkmann and Weiler, (2014) developed custom built
9 poly-ethylene (PE) probes with an equilibration chamber allowing additional mixing of the
10 vapor to prevent condensation in the sample line. They further proposed a sophisticated
11 system with a CRDS device (Picarro L2120-i, CA, USA) calibrated with standards added to
12 previously oven dried substrate from their study site.

13 In the present study in-situ usability of commercially available PP-membranes (BGL-30,
14 Umweltmesssysteme, Munich) using a liquid water analyzer (Los Gatos Research, DLT-100)
15 for a determination of stable isotopes in soil pore water is demonstrated. The proposed system
16 is applied under harsh remote field conditions in a semi-arid environment in soil with
17 moisture contents ranging from 0.3 to 6 %. In comparison to earlier in-situ studies this study
18 presents I.) an improved automatization with minimal technical modification of commercially
19 available parts. II.) We demonstrate that in-situ measurements are comparable to data derived
20 from cryogenic vacuum extractions. But also, that there are differences at the transition to the
21 atmosphere which will be discussed. Such a comparison seems to be useful since the
22 cryogenic soil water extraction allows a direct determination of the soil water isotopic
23 composition. III.) Finally, derived isotope data is used quantitatively to determine the soil
24 water balance of a deep sandy unsaturated zone and for the partitioning of transpiration and
25 evaporation.

26

27 **2 Study Site and Methods**

28 The study area is located in northern central Namibia and is part of the Cuvelai-Etosha-Basin
29 (CEB). The whole surface water catchment has an extent of about 173,000 km² where the
30 northern part (approx. 52,000 km²) belongs to Angola and the southern part to Namibia. This
31 sedimentary basin is divided into four major sub-basins called Iishana, Niipele, Olushandja
32 and Tsumeb and can be further separated into different drainage zones. Measurements were

1 conducted within the eastern sand zone close to the township of Elundu as indicated in Figure
2 1. The assignment of the catchment and its sub-basins is based on geography, population
3 distribution and water infrastructure (Dragnich et al., 2004). The main shallow aquifer system
4 in the CEB is a multilayer aquifer system in the Andoni formation with a thickness of 6 to 80
5 m. The main groundwater flow is towards the Etosha pan with an average gradient of 0.2 %
6 (Christelis and Struckmeier, 2001). Beside the shallow aquifer, recent studies identified an
7 area of 500 km² potentially containing fresh groundwater at a depth of 200 m namely the
8 Ohangwena II aquifer (Lindenmaier and Christelis, 2012; Lindenmaier et al., 2014).
9 Groundwater recharge mechanisms concerning both, the shallow and the deep aquifer are not
10 yet fully understood. The shallow aquifer system consists partly of freshwater lenses on
11 brackish to saline groundwater mostly in the Iishana region. Perched discontinuous aquifers
12 are found in the eastern part of the basin they develop on clay lenses in the subsurface and are
13 managed through hand-dug wells.

14 The climate in the CEB is semi-arid with a rainy season lasting from November to April and a
15 dry season from May to October. Annual average potential evaporation can reach up to 3,000
16 mm and decreases slightly from north to south (Mendelsohn et al., 2013). Annual average
17 rainfall ranges between 250 and 600 mm, most of the rain is falling in January and February
18 (Mendelsohn et al., 2013). The eastern part of the catchment receives more consistent rainfall
19 whereas rain in the western part is less predictable.

20 The investigated site is forested, predominantly vegetated with *Combretum collinum*, *Acacia*
21 *erioloba* and *Baikiea plurijuga*. The deep Kalahari sand can reach a depth of over 40 meters
22 and has high saturated hydraulic conductivity (2304 – 2409 cm day⁻¹) determined with
23 double-ring infiltration experiments, high porosity (0.4) and low field capacity (~ 3.5 %).
24 Sampling and measurements were conducted during two field campaigns. The first field
25 campaign was carried out between June 9th and 15th, 2014 and the second between November
26 15th and 22nd, 2014. To determine heterogeneity of infiltration and evaporation processes and
27 to evaluate an in-situ approach determining stable isotopes in soil water nine plots within an
28 area of 9,000m² were investigated. During the first campaign soil gas probes were installed at
29 depths of 2, 5, 10, 15, 20, 25, 30, 40 and 50 cm. Two plots were established with different
30 vegetation characteristics such that one was vegetated with shrubs and the other was exposed
31 without any vegetation. During the second field campaign probes were installed at depths of
32 2, 5, 7.5, 10, 12.5, 15, 17.5, 20, 25, 30, 40, 50, 60, 70, 80, 90 and 100 cm to reach a maximum

1 resolution especially for the top layer. Soil moisture measurements were conducted with a
2 time domain reflectrometry system (TDR, EasyTest, Poland) at the beginning of each
3 measurements cycle with the same resolution. In addition to the in-situ measurements samples
4 were collected in head space glass vials, crimp sealed to avoid evaporation and the soil water
5 extracted in the laboratory. Samples were transported via aircraft to the laboratory of the
6 Federal Institute of Geosciences and Natural Resources (BGR) in Hannover, Germany.

7 In the laboratory grain size analyses was conducted on 10 g soil material from the extracted
8 soil samples with the method proposed by Altuhafi et al. (2013). Soil water was extracted
9 cryogenically using a slightly modified method of the cryogenic-vacuum extraction described
10 by Koeniger et al., (2011). A custom built isolated aluminium block is heated to 105 °C
11 instead of a water bath. The sample vials are entered into the hot aluminium block to
12 evaporate the water sample. Each sample was evacuated at -3 mbar vacuum and extracted for
13 15 min. The extracted water samples were subsequently measured with a cavity ring-down
14 spectrometer (CRDS, model L2120-i, manufactured by Picarro Inc.). $^{18}\text{O}/^{16}\text{O}$ and $^{2}\text{H}/^{1}\text{H}$
15 isotope ratios are normalized on the international δ - scale and expressed as parts per thousand:

$$16 \quad \delta = \left[\left(\frac{R_{\text{sample}}}{R_{\text{reference}}} \right) - 1 \right] \quad [1]$$

17 where R_{sample} (–) denotes the $^{18}\text{O}/^{16}\text{O}$ isotope ratio (respectively $^{2}\text{H}/^{1}\text{H}$) of a water sample and
18 R_{standard} (–) those of the Vienna Standard Mean Ocean Water (VSMOW) (Coplen, 2011). All
19 values where corrected for drift and memory applying the method proposed by van Geldern
20 and Barth, (2012). Accuracies for long-term quality check standards are better than 0.2 ‰ and
21 0.8 ‰ for water samples, but an additional error for sandy soils needs to be considered which
22 can be better than 0.8 ‰ and 4 ‰ for $\delta^{18}\text{O}$ and $\delta^2\text{H}$, respectively as suggested by Königer et
23 al. (2011). The standard deviation determined from replicate samples (three per extracted soil
24 sample) is used as an additional analytical error. Subscripts are used to distinguish between
25 either the in-situ (I) and the cryogenically (C) derived isotope values in the remaining text.

26 For the determination of $\delta^2\text{H}_I$ and $\delta^{18}\text{O}_I$, commercially available soil gas probes (BGL-30,
27 Umweltmesssysteme, Munich (UMS)) with a diameter of 9.4 mm and a length of 300 mm
28 were connected to an integrated cavity off-axis liquid water isotope analyser (OA-ICOS, Los
29 Gatos research, DLT100). This device does not measure continuously and it is mandatory to
30 maintain the response from the laboratory autosampler, which is here done via the RS-232
31 interface of a Laptop computer and a computer code that responds to the requests of the laser

1 spectrometer (Figure 2). Each soil gas probe is separated from the main transport line with a
2 valve (Clippard Minimatic, USA). The valves are switched by a high or low signal from the
3 data terminal ready (DTR) and request to send (RTS) pins of the modified USB-to-RS232
4 converter. A reduction of the electric tension output of the converter is necessary which is
5 done using a resistor with $220\ \Omega$. To secure the converter against inverse currents a common
6 diode is installed in reverse direction before the optocoppler (ULN2303). The optocoppler is
7 necessary to ensure the +12 V power supply. To avoid over heating of the analyser during day
8 time by direct sun radiation a gazebo was positioned above the loading area of the pick-up
9 truck where the analyser is mounted. Power supply of the entire system was maintained using
10 a common 230 V generator.

11 Four repetitive measurements at each depth were performed during the first campaign. During
12 the second campaign six consecutive measurements were performed at each depth. A
13 measurement cycle consists of three steps: i.) a flushing phase where the cavity is evacuated,
14 ii.) the sample intake opening a particular valve and iii.) the measurement of the sample.
15 Flushing introduces a vacuum of 0.1 torr or less. The sample intake is controlled by valves
16 which are opened for 10 s for each measurement allowing a volumetric flow rate between 95
17 and 110 ml/min. The transported gas volume is measured with a flow rate measurement
18 device (Analyt-MTC, 0-200 ml min^{-1}). The probe and the transport lines to the analyser have
19 a volume of approximately 40 ml. The sample lines are made of steel and are connected with
20 Swagelok® connectors. After six consecutive measurements at one depth, the sampled soil
21 volume is approximately 120 ml. Assuming that the soil volume around the 300 mm long
22 probe is sampled equally over the whole length, a diameter of 1cm around the probe will be
23 directly affected by the uptake of vapor via the probe. Hence the top layer is measured with
24 reasonable accuracy for this particular setup. The measurement of a 1 m deep profile
25 considering 16 different depths with six repetitions and a resolution down to 2.5 cm for the
26 top 20 cm takes about 4.5 hours. The OA-ICOS device needs an additional warm up of about
27 two hours in order to get a reasonable precision.

28 During the second field campaign three transects are measured consisting of three plots to
29 characterize the spatio-temporal variability after two consecutive rain events. Each transect is
30 150 m in distance from each other as well as each profile within one transect. Transects
31 consist of bare plots as well as vegetated plots (Table 2). However, lateral roots could be
32 found at each plot.

1 Standard preparation is done using 200 g of previously oven dried (at 105 °C for at least 24 h)
2 sandy substrate for each of the four standards (Table 2). The dried soil material has been
3 transported in aluminium bags (WEBA bags®, Weber Packaging GmbH, Göglingen,
4 Germany) from the laboratory of the University of Windhoek to the field site and were then
5 spiked directly in the field with a volume of 5 ml standard before the experiment at the day of
6 measurement. Normalization to the international scale is done using one low standard
7 (HGLA) and one high standard (HMER). In addition one standard for drift correction (HDES)
8 and a quality check standard (HLAU) were used. The quality check standard is a water of
9 known isotopic composition that is treated as an unknown sample. The difference between
10 that known value and those measured expresses the accuracy of the measurement. All
11 standards were measured at the beginning of each experimental sequence; additionally HDES
12 and HLAU were measured at the end of each sequence. Isotope values of the used standards
13 are illustrated in Table 1. The standards were used only for two consecutive measurement
14 series and then new standards were prepared. Calibration standards were kept in flasks with a
15 diameter of 2 cm and a length of 50 cm. Soil gas probes were subsequently entered and the
16 flasks sealed to avoid evaporation.

17 **Soil water balance**

18 Recharge rates were determined in mm/y using a simple empirical relationship applied to the
19 data of the deep isotope depth profile (> 4 m). Therefore the difference between the deuterium
20 excess of the LMWL and the intercept of the linear regression to isotope data of deep soil
21 water is defined as $\delta^2\text{H}_{\text{shift}}$. This relationship is proposed by Allison et al., 1984 and for $\delta^2\text{H}$
22 given here as in Clark and Fritz, (1997):

$$23 R = \left[\frac{22}{\delta^2\text{H}_{\text{shift}}} \right]^2 \quad [2]$$

24 and for $\delta^{18}\text{O}$

$$25 R = \left[\frac{3}{\delta^2\text{O}_{\text{shift}}} \right]^2 \quad [3]$$

26 Assuming steady state soil evaporation is calculated from the isotope depth profiles using an
27 analytical solution (Allison et al., 1984).

$$1 \quad E = (1 - h_a)N_{sat} \tau D^v \frac{(p - \theta_v)}{\rho z_{ef}} \quad [4]$$

2 Thus, evaporation can be determined providing the relative humidity h_a [-], the saturated
 3 water vapor pressure N_{sat} [hPa], the tortuosity with $\tau=0.67$ [-], the diffusivity of water
 4 vapor in air $D^v = 24 * 10^{-6}$ [$m^2 s^{-1}$], the density of water ρ [$kg m^{-3}$], the porosity p and
 5 the soil water content θ_v [$m^3 m^{-3}$]. Calculations were conducted for a mean ambient
 6 temperature of 20 °C and 50 % relative air humidity and further with 27 °C and 60 % for
 7 Campaign 1 and Campaign 2, respectively. The depth of the evaporation front z_{ef} can be
 8 determined by an exponential fit to the isotope depth profiles (Allison et al., 1985).

$$9 \quad \delta = \delta_{res}(\delta_{ef} - \delta_{res})exp^{-z/z_{ef}} \quad [5]$$

10 The data of the isotope depth profile δ is calculated from the fitted parameters z_{ef} , the isotope
 11 value of the reservoir δ_{res} and the isotope ratio at the evaporating front δ_{ef} . This will give a
 12 quantitative estimation of the soil water balance based on the presented isotope data. In
 13 addition z_{ef} is determined from grain the grain size distribution as follows (Or et al., 2013):

$$14 \quad z_{ef} = \frac{2\alpha}{\rho g \left(\frac{1}{r^1} - \frac{1}{r^2} \right)} \quad [6]$$

15 with the surface tension of water α calculated at 24 °C, the minimum r^1 and the maximum r^2
 16 grain size of the soil.

17 **3 Results**

18 **Campaign 1**

19 The first field campaign was conducted shortly after the rainy season. No rain occurred during
 20 that campaign. The texture (medium sand) was uniform throughout the depth profile. No
 21 changes in texture were observed for the other investigated plots. Temperature and humidity
 22 variability within the sampling period between daytime (~30 °C_{max} and 15 %_{min}) and night (~
 23 9 °C_{min} and ~ 90 %_{max}) was high during the first campaign.

24 During the first campaign (June 15th, 2014) measurements were taken at two plots (E1.1,
 25 E1.2) at a distance of 25 meters on the same day. The measurement at E1.1 started at 09:30
 26 and later at 16:00 at plot E1.2. Plot E1.1 was not vegetated and had a thin soil crust in the top
 27 first centimeter. Volumetric water content increased from 0.3 % at the top to 4.1 % at 50 cm
 28 depth (Figure 3, left). Plot E1.2 was vegetated, a dense root mat was visible in the upper 10

1 cm. In contrast to E1.1 water contents were much lower increasing from 0.3 % at the surface
2 to 0.7 % at 50 cm depth (Figure 3, center). The isotope depth profiles were of similar shape
3 and magnitude for both profiles with a maximum at 10 cm and an exponential decline down
4 to the maximum depth. Due to low water contents in the upper 15 cm of the vegetated plot,
5 not enough water could be extracted with the cryogenic extraction method. However, at 10
6 cm depth the same pattern as for profile E1.1 could be observed. The shape of the isotope
7 depth profiles was different for $\delta^{18}\text{O}$ and $\delta^2\text{H}$ within the upper 5 to 10 cm. For instance, the
8 maximum isotope values of $\delta^2\text{H}_c$ and $\delta^{18}\text{O}_c$ were at 15 cm. In contrast, the maximum isotope
9 values of $\delta^2\text{H}_i$ and $\delta^{18}\text{O}_i$ were at 10 cm.

10 As depicted in Figure 4, the deuterium excess for both profiles showed a maximum at 10 cm
11 depth and exponentially declines down to 50 cm. At the vegetated plot deuterium excess
12 values were positive within the top 7.5 cm. Comparing deuterium excess values of the
13 cryogenic extraction with those from the in-situ measurements, it could be found that they
14 agree well for the bare soil plot, but not at 10 cm and 15 cm depth. In contrast, all values
15 measured in the field below 10 cm of the vegetated plot, which had very low water contents
16 (< 1 %), were shifted towards more positive values indicating less evaporative enrichment. In
17 comparison to the isotope depth profiles the deuterium excess depth profile has its minima at
18 10 cm for both methods excluding profile E2.7.

19 **Campaign 2**

20 During the second campaign variations in temperature and humidity were much smaller
21 compared to Campaign 1 (daytime $\sim 35\text{ }^\circ\text{C}_{\text{max}}$ and $30\text{ \%}_{\text{min}}$; night $\sim 20\text{ }^\circ\text{C}_{\text{min}}$ and $\sim 90\text{ \%}_{\text{max}}$).
22 Two rainfall events were recorded (November 12nd, 2014: 12 mm morning, November 13rd,
23 2014, 30 mm morning) at the climate station in Eenhana which is approximately 15
24 kilometers west of the experimental site. However, there is no isotope data available until
25 November 17th, 2014. Later during the campaign a small rain event (16 mm) could be
26 sampled for isotopes on November 17th, 2014 at 8:00 a.m. with $-0.6\text{ \textperthousand}$ and $3.0\text{ \textperthousand}$ for $\delta^{18}\text{O}$
27 and $\delta^2\text{H}$, respectively. A smaller event (4 mm) could be sampled at November 19th, 2014 with
28 isotope values of $3.6\text{ \textperthousand}$ and $28.8\text{ \textperthousand}$ for $\delta^{18}\text{O}$ and $\delta^2\text{H}$. Both events are indicated in Figure 7
29 by a grey dot on the x-axis.

30 The plots that were sampled in November (rainy season) have higher water contents
31 compared to those of the first campaign. One non-vegetated plot of the second campaign

1 (E2.7, see Fig. 4 right hand side and Table 2) is used to compare the in-situ and the laboratory
2 results as an example with higher water contents. The water contents range between 4.4 %
3 and 6.8 % with maximum values between 12.5 cm and 25 cm (Figure 3, right). Strongest
4 enrichment of $\delta^{18}\text{O}$ is in the top layer declining exponentially with depth for both methods.
5 There is good agreement between $\delta^{18}\text{O}_I$ and $\delta^{18}\text{O}_C$ except for the depth at 30 cm and 50 cm. In
6 contrast, there are substantial differences between $\delta^2\text{H}_I$ and $\delta^2\text{H}_C$. Above 25 cm values of $\delta^2\text{H}_C$
7 are higher (-15.5 ‰ to -22.6 ‰) than for $\delta^2\text{H}_I$ (-25.0 ‰ to -29.2 ‰), and vice versa lower
8 below 25 cm with -23.4 ‰ to -15.2 ‰ for $\delta^2\text{H}_C$ and -11.6 ‰ to -5.1 ‰ for $\delta^2\text{H}_I$, respectively.

9 There is a good agreement between in-situ and cryogenically obtained isotope measurements
10 for both isotope depth profiles of the first campaign between 15 and 50 cm (RMSE= 3.9 and
11 9.2 ‰ for $\delta^{18}\text{O}$ and $\delta^2\text{H}$, respectively). However, higher values were observed for the in-situ
12 approach at shallower depth (RMSE= 7.0 and 43.4 ‰ for $\delta^{18}\text{O}$ and $\delta^2\text{H}$, respectively). In
13 general, better agreement can be observed for $\delta^{18}\text{O}$ compared to $\delta^2\text{H}$ values. Both isotope
14 profiles of the first campaign derived from the cryogenic vacuum extraction show a maximum
15 at 15 cm with an exponential decline down to depth. Values of the in-situ measurement show
16 this maximum at 10 cm, but only for $\delta^{18}\text{O}_I$. The profile of the second campaign does show
17 good agreement within the top 25 cm for $\delta^{18}\text{O}_I$ but for $\delta^2\text{H}$ only within the upper 10 cm. In
18 terms of accuracy for the set of these three profiles we obtain 6.86 ‰ and 1.87 ‰ for $\delta^2\text{H}_I$ and
19 $\delta^{18}\text{O}_I$, respectively.

20 A compilation of the quality check standards for $\delta^2\text{H}_{qc}$ and $\delta^{18}\text{O}_{qc}$ of the two campaigns is
21 shown in Table 2. The standard deviation of the repetitive measurements for each depth is a
22 measure of measurement precision. After drift correction and normalisation of the isotope
23 depth profile E1.1 the precision (σ_{qc}) of the quality check standard (HLAU) was 5.2 ‰ $\delta^2\text{H}$
24 and 0.66 ‰ $\delta^{18}\text{O}$, respectively. The mean precision of the repetitive measurements (σ_{rep}) is
25 two times better for $\delta^2\text{H}_I$ than for the precision of the repetitive measurements (σ_{cry}) for values
26 derived with the cryogenic vacuum extraction $\delta^2\text{H}_C$. Values of $\delta^{18}\text{O}_{qc}$ show a higher similarity
27 (refer to Table 2). The measurement of the second profile E1.2 is less precise for $\delta^2\text{H}_I$ but in
28 the same range as $\delta^2\text{H}_C$. Similar precision as for profile E1.1 is found for the third profile E2.7
29 for both $\delta^2\text{H}$ and $\delta^{18}\text{O}$, respectively.

30

31 **$\delta^{18}\text{O}$ vs $\delta^2\text{H}$**

1 In Figure 5 the $\delta^{18}\text{O}$ to $\delta^2\text{H}$ relationship is shown. The LMWL is derived from historical data
2 collected in the CEB and has a slope of 7.3 ($R^2 = 0.96$). Additionally, mean values of local
3 groundwater ($\sigma^{18}\text{O} = 0.91$, $\sigma^2\text{H} = 4.27$) and soil water down to a depth of 4 m with 10 cm
4 resolution are presented. Soil water from the first field campaign derived from the cryogenic
5 vacuum extraction plots along an evaporation line with a slope of 2.4 ($R^2 = 0.79$) for the non-
6 vegetated plot and 3.1 ($R^2 = 0.96$) for the vegetated plot. In-situ measurements of the non-
7 vegetated plot have a slope of 3.9 ($R^2 = 0.84$). Excluding the first 10 cm of the unvegetated
8 profile the slope is 2.9 ($R^2 = 0.73$). Values of the vegetated site derived from the in-situ
9 measurements have a slope of 3.0 ($R^2 = 0.46$) and are shifted towards more positive $\delta^2\text{H}$ values.
10 Excluding the top 15 cm of the in-situ measurement the slope remains the same but R^2
11 increases to 0.9. Values from the second campaign show a much higher slope with 5.3 ($R^2 =$
12 0.75) for the in-situ measurement and 5.1 ($R^2 = 0.96$) for the cryogenic vacuum extraction and
13 are plotting close to the LMWL.

14 **Spatio-temporal variability**

15 Each profile of the second campaign is measured at 18 different depths and each depth with
16 six repetitions. After drift correction of the isotope data, the mean precision considering the
17 quality check measurements (σ_{qc}) for more than 140 measurement points is 2.15 ‰ for $\delta^2\text{H}_I$
18 and 0.36 ‰ for $\delta^{18}\text{O}_I$ (Table 2). Mean standard deviation of the repetitive measurements (σ_{rep})
19 of each depth is 1.86 ‰ for $\delta^2\text{H}_I$ and 0.46 ‰ for $\delta^{18}\text{O}_I$, respectively. As shown in Table 2, the
20 mean standard deviations of the repetitive measurements are similar to those derived from the
21 quality check standard. Differences are observed between σ_{qc} and σ_{rep} . However, the precision
22 of $\delta^2\text{H}$ is within the range of the mean accuracy of 5.1 ‰. The accuracy of $\delta^{18}\text{O}$ is much
23 higher with 0.11 ‰. There are two outliers (E2.8, E2.9) who were not considered for the
24 mean precision nor for the mean accuracy.

25 Mean values of each transect are shown to illustrate an averaged temporal characteristic with
26 intermittent rainfall (Figure 6) for this particular area. The first transect is affected only from
27 the first set of rain events (E2.1 to E2.3) and was measured within two consecutive days. The
28 next transect (E2.4 to E2.6) is affected by the 16 mm event (17th November, 2014) of which
29 isotope data is available and the profiles were measured in a period of three days. Finally, the
30 last three plots (E2.7 to E2.9) showed most evaporative enrichment and experienced only
31 additional precipitation on the 19th Nov 2014 with an amount of 4 mm. Maximum infiltration
32 depth varied between 65 and 95 cm. Water content varied between 0.5 % and 9.5 %.

1 Comparing the three transects it can be observed that variability of isotope depth profiles
2 decreases from the first to the last transect and an evaporation profile developed.

3 To account for spatial variability mean values of soil moisture were calculated for each depth
4 of the nine plots. Additionally, the standard deviation of each depth for soil moisture, $\delta^{18}\text{O}$
5 and $\delta^2\text{H}$ are calculated. Figure 7 shows mean soil moisture of each depth against the standard
6 deviation of soil moisture and those of the two isotopes. Basically, high ($> 4\%$) and low ($< 2\%$)
7 water content have lower variability of soil moisture compared to intermediate values. In
8 contrast, the standard deviation of $\delta^{18}\text{O}$ and $\delta^2\text{H}$ increases with decreasing soil water content.

9 **Soil water balance**

10 Precipitation (P) for the rainy season was measured with an amount of 660 mm. Recharge
11 estimated from soil water stable isotope data is less than 1 % of precipitation. It ranges
12 between $R = 4 - 5 \text{ mm y}^{-1}$ derived from $\delta^2\text{H}_{shift}$ and $\delta^{18}\text{O}_{shift}$, respectively. The soil water
13 storage (S) is derived from the soil moisture depth profile and the evaporation front is
14 determined from the exponential fit to the water stable isotope depth profiles. Results are
15 summarized in Table 3. Soil evaporation (E) is determined from z_{ef} using the isotope depth
16 profiles. The mean of all results from E1.1 and E1.2 is $120 \pm 50 \text{ mm y}^{-1}$. Then, Recharge (R),
17 soil water storage (S) and soil evaporation (E) are subtracted from precipitation (P). The
18 remainder is potentially available for transpiration (T) with $510 \pm 50 \text{ mm y}^{-1}$. Runoff can be
19 neglected because it was not observed at the experimental site. Hence, the contribution of
20 transpiration to total evapotranspiration (E/T_{pot}) is $77 \pm 7\%$. The potential contribution of
21 transpiration (E/T_{pot}) or root water uptake at the non-vegetated plot is between 76 and 92 %.
22 At the site underneath the canopy and vegetated with shrubs E/T_{pot} is between 72 and 92 %.

23 Values of z_{ef} range between 110 and 290 mm which is in agreement with values derived from
24 a physical model proposed by Or et al., (2013). Considering two different ranges, one for
25 finer and one for coarser texture, we derive a depth z_{ef} of 210 mm and 118 mm for $r^1 = 63 -$
26 $112 \mu\text{m}$ and $r^2 = 630 - 1120 \mu\text{m}$, respectively. Using these values to calculated E for profiles
27 from June 2014 we derive values between $67 - 79 \text{ mm y}^{-1}$ and $161 - 201 \text{ mm y}^{-1}$ for r^1 and r^2 ,
28 respectively.

29 After the rain events during the second field campaign the evapotranspiration pattern is
30 dominated by soil evaporation. The evaporation front is still developing ($z_{ef} = 82 - 90 \text{ mm}$)

1 and E/T_{pot} is much lower with 35 – 51 %. Applying this methodology to the different
2 transects, soil evaporation E decreases from 4 to below 1 mm d⁻¹ (not shown).

3 **4 Discussion**

4 The potential to determine stable isotopes of soil water indirectly by measuring the vapor
5 from the pore space directly in the field could be demonstrated by using a liquid water
6 analyser. Results show that the precision of the in-situ approach is better than 0.8 ‰ and 2.5
7 ‰ for $\delta^{18}\text{O}$ and $\delta^2\text{H}$, respectively. This is a feasible precision if it is compared the precision of
8 isotope values from the cryogenic vacuum extraction method which are 0.8 ‰ and 3.5 ‰ for
9 $\delta^{18}\text{O}$ and $\delta^2\text{H}$, respectively. It is still worse compared to the precision that can be achieved
10 measuring stable isotopes directly from water samples (0.2 ‰ and 0.8 ‰ for $\delta^{18}\text{O}$ and $\delta^2\text{H}$).
11 However, it needs to be considered that such laser spectrometers are in general mounted in a
12 temperature controlled laboratory. In this study, accuracy and precision of the presented in-
13 situ system is mainly limited by the environmental conditions. If the laser spectrometer and
14 the autosampler would be operated within a temperature controlled environment, possibly, the
15 precision could be improved. However, this study could demonstrate that it is possible to
16 determine stable isotopes of soil water directly in the field with a similar or even better
17 precision compared to destructive sampling and a subsequent soil water extraction in the
18 laboratory. This creates possibilities to investigate water vapor transport processes that are
19 difficult to measure with other techniques such as soil moisture or suction tension
20 measurements. Evaporation processes are physically well described (i.e. Or et al., 2013), but
21 their determination in the field remains very difficult. An approach to observe evaporation
22 was presented by Rothfuss et al. (2015) who could show the development of an isotope depth
23 profile in a drying soil column experiment with a similar in-situ approach as in the present
24 study. However, their experimental setup did not reflect conditions that can be found at our
25 study site, since much higher temperature and humidity gradients were observed between day
26 and night.

27 **Campaign 1**

28 Results of the first field campaign demonstrates good agreement of the isotope depth profiles
29 between the cryogenic vacuum extraction method and the in-situ approach for deeper parts of
30 the soil profile, but also a divergence in the top 15 cm. Differences could be a result of an
31 incomplete soil water extraction, rayleigh fractionation caused by the uptake of air from the
32 in-situ measurement, natural processes or natural heterogeneity.

1 An incomplete extraction of water will result in depleted isotope values of the extracted soil
2 water. However, this is unlikely for fine sand with very low water holding capacity and very
3 low abundance of silt and clay. The cryogenic vacuum extraction is capable to extract the
4 entire water in sandy soils (Königer et al., 2011). Hence, the extracted soil water isotopic
5 composition will reflect the “true” isotope values of the pore water.

6 Measuring with the soil gas probe in a very coarse material atmospheric vapor or even vapor
7 from other parts of the soil can lead to a mixed sample. However, the extracted air volume is
8 very low and a divergence of isotope values is only visible within the top 15 cm of the dry
9 profiles (Figure 3, left and center). Evaporative enrichment is reflected in the deuterium
10 excess (d_{ex}) and also in the so-called evaporation line (Craig and Gordon, 1965). Evaporative
11 enrichment could also be enhanced by the uptake of water vapor through the measurement
12 (Figures 5 and 6). The equilibrium condition prevailing between soil liquid and gas phases is
13 disturbed when water vapor is removed. Then the sampled water vapor can be depleted at
14 first. After some time, depending on the uptake rate and the soil water content, the initial
15 isotopic composition of the remaining soil water might enrich itself and isotope values in the
16 sampled gas will become more enriched. This effect might be reflected in a reduced precision.
17 However, enrichment caused by the uptake of air through the measurement is not visible for
18 deeper parts of profile E1.2 which is very dry as well. Hence, arguing with low water contents
19 would suggest to have enriched values for deeper parts of the vegetated profile. This is not
20 observed at the vegetated plot where soil water contents are below 1% throughout the whole
21 profile (Figure 3, center). Since the in-situ approach is based on the same principle as the
22 equilibration bag method its applicability on samples with low water content is supported by a
23 recent study of Hendry et al., (2015). They found that the accuracy of their equilibration
24 procedure could be improved by increasing the sample amount.

25 Beside this, it has to be noted that destructive sampling was conducted one day after the in-
26 situ measurements because it was assumed that the isotope profiles are in steady state (Barnes
27 and Allison, 1988), and the experimental setup did not allow for simultaneous sampling.
28 Therefore, the observed differences in the upper part of the soil profile might be rather
29 attributed to kinetic processes, because vapor transport (i.e. evaporation) and hence isotopic
30 enrichment will more pronounced at shallow depths as described by Braud et al. (2009).
31 Natural temporal variability such as high temperature and humidity changes between day and
32 night could be another possible explanation. During the day evaporation dries the top layer

1 due to vapor transport into the atmosphere. During the night, temperatures decrease and
2 relative humidity increases. Low soil water contents and a back diffusion of vapor into the
3 upper part of the soil might cause condensation or adsorption (Agam and Berliner, 2006),
4 affect isotope values (Rothfuss et al., 2015) and can significantly increase soil water content
5 (Henschel et al., 2008). This might deplete isotope values of the remaining soil water within
6 that upper layer. In a numerical study it was already shown that diurnal variations of
7 evaporation can be large depending on the energy budget at the surface but the influence on
8 isotope concentrations needs further investigation, especially under field conditions (Braud et
9 al., 2005).

10 Another possibility for a change in isotopic composition at shallow depths can be hydraulic
11 lift. In this case water from deeper soil layers with higher water potential can move through
12 the root system to soil layers with lower water potential (Dawson et al., 1993) The dense root
13 mat of fine roots observed in the upper part of the soil profile together with very low water
14 contents and the differences between the isotope depth profiles could be an indicator for this
15 process. However, the measurement of soil physical properties, stable isotopes of soil water
16 and xylem covering the diurnal cycle would be necessary to distinguish between either vapor
17 back diffusion or hydraulic redistribution.

18 **Campaign 2**

19 In contrast to depth profiles of the first campaign the rain influenced profile E2.7 doesn't
20 show such a divergence in the top layer as observed at E1.1 and E1.2. As shown in Figure 5
21 the deuterium excess indicates that precipitation water is dominating. Good agreement is
22 found in the top layer for both isotopologues. Mixing with atmospheric vapor might be
23 negligible considering the high soil water contents. Destructive sampling was done directly
24 before the in-situ measurement started. It has to be noted that, in-situ measurements at 10 cm
25 depth were done 90 min after the destructive sampling was conducted. In-situ measurements
26 at 30 cm depth were conducted even 120 min later. Differences can be caused by the time lag
27 between destructive sampling and in-situ measurement, vapor transport processes induced by
28 temperature gradients or diffusion.

29 Considering that under the present "wet" conditions (but also if the soil moisture is around
30 wilting point) humidity of the pore space is close to saturation. Then temperature gradients
31 will cause a movement of vapor downward and upward depending on the temperature profile

1 (Abramova, 1969). Further, soil evaporation can be separated into direct evaporation from a
2 water saturated surface (stage I evaporation) and diffusion controlled vapor transport (stage II
3 evaporation) (Or et al., 2013). Therefore, observed differences between $\delta^2\text{H}_I$ and $\delta^2\text{H}_C$ for
4 profile E2.7 (Figure , right) might be attributed to the exchange between the evaporation
5 depleted vapor that was transported from the deeper part (30 cm to 50cm) to shallower depth
6 (12.5 cm and 25 cm) due to diffusion controlled evaporation (stage II).

7 **$\delta^{18}\text{O}$ vs $\delta^2\text{H}$**

8 Values for in-situ measurements and cryogenic extraction plot on evaporation lines which are
9 similar in slope (excluding the top 12.5 cm). The outliers in the top-right area and those above
10 the LMWL of the $\delta^2\text{H}$ vs. $\delta^{18}\text{O}$ plot (Fig. 5) are from the top 12.5 cm of the profiles. As
11 discussed earlier, diurnal temperature and humidity cycles could cause i.e. condensation in the
12 upper part of the soil profile, but also higher enrichment during the daytime compared to the
13 conditions during the night when the soil is colder than the vapor in the atmosphere. Further,
14 the interaction between soil water potential and water vapor, which might be driven by
15 relative humidity (Wilson et al., 1997) but the effect to isotope fractionation, is not well
16 understood and will be a challenge to future research (Soderberg et al., 2012). The
17 investigation of such processes using in-situ approaches for stable isotope analysis seem to be
18 promising in this regard, since the composition of vapor can be measured in the field.

19 **Spatio-temporal variability**

20 The boundary conditions of the second field campaign caused a quite heterogeneous pattern
21 regarding both the development of the moisture front and the isotope depth profiles. It can be
22 observed how the infiltrating water develops under evaporation with light intermittent rainfall
23 events. This is reflected in both the shape of isotope depth profiles of the three transects and
24 the standard deviations within one transect (Figure 6). Other studies showed similar patterns
25 in the context of a numerical experiment (Singleton et al., 2004). The first transect (Figure 6,
26 Transect 1) has variable isotope values throughout the whole depth. The isotope depth profile
27 of transect one shows maxima and minima of isotope values which appear with a similar
28 shape as a profile in a humid climate. This kind of layering is commonly used in humid
29 regions to determine transit times of unsaturated zone water where precipitation has seasonal
30 different isotopic composition (Coplen et al., 2000; Lee et al., 2007). However, here it is
31 attributed to variations in rainfall composition and infiltration patterns on a much smaller time
32 scale namely daily. Zimmermann et al., (1967) previously described that isotopically distinct

1 rain that is consecutively infiltrating into the soil will move downward distinguishable by a
2 boundary between older rainwater below and younger water above. Hence, the most depleted
3 values found at 20 cm and 50 cm (Figure 6, Transect 1) might correspond to certain rain
4 events which would not emerge from the soil moisture measurements alone. These depleted
5 zones are not visible in the other transects which are possibly overprinted by vapor transport
6 processes and evaporation.

7 Short time after rains stop the top part of the evaporation profile (Transect 1) was
8 considerably displaced as theoretically described by Allison et al., (1984). Variations of
9 isotope values are attenuated with time by vapor phase redistribution (Transect 2) (Fontes et
10 al., 1986) and an evaporation profile is begins to develop (Transect 3) (Rothfuss et al., 2015).
11 Further it can be observed that infiltrating water of small intermittent events compresses the
12 isotope profile (Barnes and Allison, 1988; Singleton et al., 2004). Therefore the presented in-
13 situ measurements have great potential to visualize theoretically discussed processes with
14 feasible accuracy under natural field conditions.

15 Spatial variability of soil moisture is well known (Western et al., 2004). It can be expected
16 that also stable isotopes will distribute heterogeneous within the unsaturated zone. The
17 relationship between mean soil moisture and $\delta^2\text{H}$ does not allow a resilient conclusion
18 because of the low accuracy. However, it appears that it behaves different for $\delta^2\text{H}$ and $\delta^{18}\text{O}$
19 values compared to soil moisture. The differences might be related to vapor diffusion
20 processes or to biological processes. For instance, Dawson et al. (2002) discussed the isotopic
21 composition of different carbon and water pools. Soil respired (CO_2) will equilibrate with the
22 abundant soil water and might cause additional changes of the isotopic composition of the soil
23 pore water.

24 **Soil Water Balance**

25 The soil water balance is calculated from isotope depth profiles. The presented results are in
26 agreement with other isotope based partitioning studies. Those suggest a contribution of
27 transpiration of more than 70 % to the total evapotranspiration flux as Sutanto et al. (2014)
28 discussed in a recent review. In addition the findings from the first field campaign showed
29 that the development of the evaporation profiles appeared to be independent of leaf /
30 vegetation cover. Based on the data and calculation of this study it seems that soil cover might
31 be of minor importance for long term soil evaporation quantities.

1 Differences between the two sites of the first field campaign are small regarding the shape of
2 the isotope depth profiles. In addition, the evaporating front and the calculated evaporation
3 rates using equation 4 and equation 5 are similar for both sites. Because of the litter layer and
4 the shaded nature of plot E1.2 it could be expected that less evaporation takes place and hence
5 less enrichment and a lower deuterium excess would appear for the in-situ measurement
6 (Figure 4). However, this is not visible and suggests humidity to be the main driver for
7 isotopic enrichment as demonstrated in a numerical study by Braud et al. (2005).

8 **Potential limitations**

9 Water vapor mixing ratio dependencies (Wang et al., 2009; Sturm and Knohl, 2010; Rambo et
10 al., 2011; Aemisegger et al., 2012) are of minor importance in this study, because the water
11 content was maintained within the density of approximately $2\text{--}4 \times 10^{16}$ molecules cm^{-3} as
12 recommended by Los Gatos Research. It is assumed that small variations will be reflected in
13 the standard deviation of the measurements. Additionally, inference through organic
14 contamination is neglected in this study. However, if necessary to account for inference recent
15 efforts include calibration strategies in this regard (Wu et al., 2014). Possible fractionation
16 due to high salt concentrations or chemical reactions as observed by Oerter et al. (2014) are
17 negligible, because the cation exchange capacity (CEC) of the sand was 0.5 meq 100g^{-1} and
18 total organic carbon (TOC) 0.22 %.

19 During the second field campaign information on long term precision and spatio-temporal
20 variability was investigated. Comparing the quality check standards of the two campaigns the
21 precision within one series (σ_{rep}) of $\delta^2\text{H}$ is one-third better than the long term accuracy.
22 However, the accuracy of $\delta^{18}\text{O}$ is three times greater than the mean precision (Table 2). This
23 can likely be improved by utilizing a more sophisticated technical setup e.g. temperature
24 controlled conditions. Another reason could be the difference in the physical properties of the
25 probe pores such as the diffusivity of gas (Merlivat et al., 1979). Though there is no detailed
26 chemical data available it is unlikely that chemical properties are responsible, since the sandy
27 soil has a very low CEC. More likely are biological processes that are introduced due to the
28 sudden availability of water. Nevertheless, there is no data (i.e CO_2 measurements) available
29 to support this assumption. Therefore, it would be beneficial to measure CO_2 concentration in
30 parallel. However, the precision appears to be sufficient to monitor processes of a diurnal time
31 scale and also comparable to other systems that were tested in the field, e.g., Volkmann and
32 Weiler et al. (2014) with values of 2.6 ‰ and 0.38 ‰ for $\delta^2\text{H}$ and $\delta^{18}\text{O}$, respectively.

1 Condensation within the sample system can lead to unreliable data. This can be either
2 prevented by heating the sample lines, flushing the sample lines with dry air or sufficient
3 dilution of the sample. Thus, under conditions where the ambient temperature is significant
4 warmer then the soil temperature a simple valve controlled membrane inlet will be sufficient
5 for an indirect determination of isotopes in unsaturated zone or saturated zone water. During
6 day time this is the case at the presented study site, but changes drastically overnight as
7 described. Dilution of the vapor concentration can be done by providing dry gas at the other
8 end of the available probes. In the case of pure diffusion sampling the maximum dilution rate
9 depends upon the absolute amount of water molecules in the vapor and is controlled by the
10 length of the probe, their diffusion properties, the flow velocity and the temperature at depth.
11 The flow velocity can be different depending on the laser spectrometer that is used. Adding a
12 mixing chamber at the head of the probe has the distinct advantage of additional mixing
13 directly before the vapor enters the sample line (Volkmann and Weiler, 2014). This leads to
14 independence on flow velocity, probe length and membrane diffusion properties with regard
15 to the water content of the sampled vapor. Under very dry conditions it might be useful to
16 increase the probe length, since the soil volume around the probe affected by the measurement
17 will be reduced.

18 A critical point is the long term application of membrane based methods. The pore space of
19 the probes can be altered over time which might increase the memory effect of the system.
20 Further, the calibration of the in-situ methods of Volkmann and Weiler (2014) and Gaj et al.
21 (this study) used prior oven dried substrate for the calibration. This procedure assumes that all
22 water is evaporated during oven drying and only the added standard water will be measured
23 afterwards. The same assumption is made using the equilibration bag method if the standards
24 are treated in the same way as described. However, interlayer water or adsorbed water of clay
25 minerals is commonly removed under vacuum heating the sample to 200 to 300 °C for several
26 hours (VanDeVelde and Bowen, 2013). These adsorbed and interlayer water is bound on the
27 mineral surface and exchanges with atmospheric water vapor within hours (Savinand and
28 Epstein, 1970). Hence, for soils containing clay minerals a calibration procedure using
29 previosly oven dried soil materials might mislead. The presented direct comparison of the
30 cryogenic vacuum extraction with a membrane based in-situ measurement showed that this
31 calibration procedure is at least applicable for fine sand. However, it will probably lead to
32 insufficient data applying this calibration procedure to soil samples with finer texture,
33 especially if clay, silt and/or salt contents are high (Oerter et al., 2014).

1 **5 Conclusion**

2 The present study demonstrates that high resolution in-situ sampling of stable isotopes in the
3 unsaturated zone is feasible. In-situ measurements can be applied with minimal technical
4 effort for remote applications. They further show good agreement with values derived from
5 cryogenic soil water extractions. Differences between the two methods are predominantly
6 within the given accuracies of the methods. Divergence in the upper soil layer between in-situ
7 and destructive sampling suggest enhanced soil-atmosphere interactions, kinetic processes
8 due to high evaporation rates or hydraulic redistribution. Evaporation induced by the
9 measurement procedure might decrease the precision depending on the uptake rate and the
10 soil water content. However more important, to prevent the collection of insufficient data
11 applying an in situ approach one has to carefully consider the applied calibration procedure
12 depending on the research question and the soil type. In addition, there is a trade-off between
13 technical effort, control setup, probe type, environmental conditions and costs.

14 Low humidity in relation to soil water potential and isotope fractionation needs further
15 investigation. Long term accuracy within the presented campaigns is about two times lower
16 for $\delta^2\text{H}$ and three times for $\delta^{18}\text{O}$ than for the short term precision of each profile. This can
17 possibly be improved by a better temperature control of the analyser or temperature
18 compensated devices if available.

19 The presented and also other in-situ measurement approaches have great potential to
20 investigate transient processes within the unsaturated zone. This has not been possible to
21 study until field deployable laser spectrometer and in-situ techniques became available. The
22 determination of water stable isotopes in the unsaturated zone directly in the field allows
23 monitoring transient processes which would not be possible with destructive sampling
24 strategies. This creates new possibilities to the design of tracer experiments with water of
25 different isotopic composition as conservative tracer. However, this is limited by the
26 measurement frequency of the provided system which is now at least able to capture diurnal
27 processes with the presented vertical resolution. In addition, a much higher spatial resolution
28 can be achieved with much lower time consumption compared to conventional approaches.
29 The proposed technique offers the possibility to investigate unsolved questions regarding soil
30 atmosphere interactions such as water vapor intrusion and transport plus effects of diurnal
31 evaporation cycling on isotope depth profiles.

1 **Acknowledgements**

2 This work was partly funded by the German Federal Ministry for Education and Research
3 (BMBF) within the SASSCAL project (South African Science and Service Center for Climate
4 Change, Agriculture and Landuse) under contract number 01LG1201L. We wish to thank our
5 colleagues Martin Quinger (BGR), Christoph Lohe (BGR), Shoopi Ugulu, and Wilhelm
6 Nuumbembe from University of Namibia, Windhoek, Namibia. Laboratory work was
7 supported by Jürgen Rausch and Lisa Brückner which is highly acknowledged. Also
8 appreciated is the technical support of Axel Lamarter, Marc Brockmann, Erik Lund and
9 Salome Krüger as well as Chris Gabrielli for proof reading.

10

1 **6 References**

2 Abramova, M. M.: Movement of moisture as a liquid and vapor in soils of semi-deserts,
3 Internat. Assoc. Sci. Hydrol., Proc. Wageningen Symposium (83), 781–789, 1969.

4 Aemisegger, F., Sturm, P., Graf, P., Sodemann, H., Pfahl, S., Knohl, A., and Wernli, H.:
5 Measuring variations of δ 18O and δ 2H in atmospheric water vapor using two commercial
6 laser-based spectrometers: an instrument characterisation study, Atmos. Meas. Tech. (5),
7 1491–1511, doi:10.5194/amt-5-1491-2012, 2012.

8 Agam, N. and Berliner, P. R.: Dew formation and water vapor adsorption in semi-arid
9 environments - A review, Journal of Arid Environments (4), 572–590,
10 doi:10.1016/j.jaridenv.2005.09.004, 2006.

11 Allison G.B., Barnes, C. J., Hughes M.W., and Leaney, F. W.: Effect of climate and
12 vegetation on oxygen-18 and deuterium profiles in soils, Int. Symp. Iso. Hydrol. Water
13 Resour. Dev., 105–123, 1984.

14 Allison G.B., Barnes, C.J., Hughes M.W.: Estimation of evaporation from the normally "dry"
15 lake frome in south Australia, Journal of Hydrology (78), 229–242, 1985.

16

17 Allison, G. B., Colin-Kaczala A.F., and Fontes Ch.J.: Measurement of Isotopic Equilibrium
18 between Water, Water Vapor and Soil CO₂ in Arid Zone Soils, Journal of Hydrology (95),
19 131–141, 1987.

20 Allison, G. B., Gee, G., and and Tyler, S. W.: Vadose-Zone Techniques for Estimating
21 Groundwater recharge in Arid and Semiarid Regions, Soil Sci. Soc. Am. (58), 6–14, 1994.

22 Allison, G. B. and Hughes, M. W.: The use of natural tracers as indicators of soil-water
23 movement in a temperate semi-arid region, Journal of Hydrology (60), 157–173, 1983.

24 Altuhafi, F., O'Sullivan, C., and Cavarretta, I.: Analysis of an Image-Based Method to
25 Quantify the Size and Shape of Sand Particles, J. Geotech. Geoenviron. Eng., 139 (8), 1290–
26 1307, doi:10.1061/(ASCE)GT.1943-5606.0000855, 2013.

27 Barnes, C. J. and Allison, G. B.: Tracing of Water Movement in the unsaturated zone using
28 stable isotopes of hydrogen and oxygen, Journal of Hydrology (100), 143–176, 1988.

1 Braud, I., Bariac, T., Biron, P., and Vauclin, M.: Isotopic composition of bare soil evaporated
2 water vapor. Part II: Modeling of RUBIC IV experimental results, *Journal of Hydrology*, 369
3 (1-2), 17–29, doi:10.1016/j.jhydrol.2009.01.038, 2009.

4 Braud, I., Bariac, T., Vauclin, M., Boujamaoui, Z., Gaudet, J. P., Biron, P., and Richard, P.:
5 SiSPAT-Isotope, a coupled heat, water and stable isotope (HDO and $H_2^{18}O$) transport model
6 for bare soil. Part II. Evaluation and sensitivity tests using two laboratory data sets, *Journal of*
7 *Hydrology* (309), 301–320, doi:10.1016/j.jhydrol.2004.12.012, 2005.

8 Caldwell, M. M., Dawson, T. E., and Richards, J. H.: Hydraulic lift: consequences of water
9 efflux from the roots of plants, *Oecologia*, 113 (2), 151–161, doi:10.1007/s004420050363,
10 1998.

11 Christelis, G. and Struckmeier, W.: Groundwater in Namibia: an explanation to the
12 Hydrogeological Map, 2011st ed., 2001.

13 Clark, I. D. and Fritz, P.: Environmental Isotopes in Hydrogeology, Lewis Publishers, 1997.

14 Craig, H.: Isotopic Variations in Meteoric Waters, American Association for the
15 Advancement of Science (133), 1961.

16 Coplen, T. B.: Guidelines and recommended terms for expression of stable-isotope-ratio and
17 gas-ratio measurement results, *Rapid Commun. Mass Spectrom.*, 25 (17), 2538–2560,
18 doi:10.1002/rcm.5129, 2011.

19 Coplen, T., Herczeg, A., and Barnes, C.: Isotope Engineering—Using Stable Isotopes of the
20 Water Molecule to Solve Practical Problems, in: *Environmental Tracers in Subsurface*
21 *Hydrology*, Springer US, 79–110, doi: 10.1007/978-1-4615-4557-6_3, 2000.

22 Dawson, T. E.: Hydraulic lift and water use by plants: implications for water balance,
23 performance and plant-plant interactions, *Oecologia* (95), 565–574, 1993.

24 Dawson, T. E.: Determining water use by trees and forests from isotopic, energy balance and
25 transpiration analyses: the roles of tree size and hydraulic lift, *Tree Physiology* (16), 263–272,
26 1996.

27 Dawson, T. E. and Ehleringer, J. R.: Streamside trees that do not use stream water, *Nature*,
28 350 (6316), 335–337, 1991.

1 Dawson, T. E., Mambelli, S., Plamboeck, A. H., Templer, P. H., and TU, K. P.: Stable
2 Isotopes in Plant Ecology, *Annu. Rev. Ecol. Syst.*, 33 (1), 507–559,
3 doi:10.1146/annurev.ecolsys.33.020602.095451, 2002.

4

5 Dincer, T., Al-Mugrín, A., and Zimmermann, U.: Study of the infiltration and recharge
6 through the sand dunes in arid zones with special reference to the stable isotopes and
7 thermonuclear tritium, *Journal of Hydrology*, 23 (1-2), 79–109, doi:10.1016/0022-
8 1694(74)90025-0, 1974.

9 Dragnich, P. A., Dungca, A. C., Pedleton Noah, L., and Tracy, A. R.: The Cuvelai-Etosha
10 Basin Management Approach; Assessing water resources management in the Iishana sub-
11 basin), 2004.

12 Dubbert, M.; Cuntz, M. M.; Piayda, A.; Maguàs; Werner, C.: Partitioning evapotranspiration -
13 Testing the Craig and Gordon model with field measurements of oxygen isotope ratios of
14 evaporative fluxes (496), 142–153, doi:10.1016/j.jhydrol.2013.05.033, 2013.

15 Ehleringer, J. R. and Dawson, T. E.: Water uptake by plants: perspectives from stable isotope
16 composition, *Plant Cell Environ*, 15 (9), 1073–1082, doi:10.1111/j.1365-
17 3040.1992.tb01657.x, 1992.

18 Fontes, J., Yousfi, M., and Allison, G. B.: Estimation of long-term, diffuse groundwater
19 discharge in the northern Sahara using stable isotope profiles in soil water, *Journal of
20 Hydrology* (86), 315–327, 1986.

21 Garvelmann, J., Külls C., and Weiler M.: A porewater-based stable isotope approach for the
22 investigation of subsurface hydrological processes, *Hydrol. Earth Syst. Sci.* (16), 631–640,
23 doi:10.5194/hess-16-631-2012, 2012.

24 Gazis, C. and Feng, X.: A stable isotope study of soil water: evidence for mixing and
25 preferential flow paths, *Geoderma*, 119 (1-2), 97–111, doi:10.1016/S0016-7061(03)00243-X,
26 2004.

27 Hendry, M. J., Schmeling, E., Wassenaar, L. I., Barbour, S. L., and Pratt, D.: Determining the
28 stable isotope composition of pore water from saturated and unsaturated zone core:
29 improvements to the direct vapor equilibration laser spectrometry method, *Hydrol. Earth Syst.
30 Sci.*, 19 (11), 4427–4440, doi:10.5194/hess-19-4427-2015, 2015.

1

2 Henschel, J. R. and Seely, M. K.: Ecophysiology of atmospheric moisture in the Namib
3 Desert., Atmospheric Research, 87 (87), 362–368, doi:10.1016/j.atmosres.2007.11.015,
4 2008.

5 Herbstritt, B., Grahler B., and Weiler M.: Continuous in situ measurements of stable isotopes
6 in liquid water, Water Resour. Res. (48), doi:10.1029/2011WR011369, 2012.

7 Herczeg, A. L., & Leaney, F. W. (2011). Review: environmental tracers in arid-zone
8 hydrology. *Hydrogeology Journal*, 19(1), 17-29.

9 Kelln, C., Wassenaar L.I., and Hendry, M. J.: Stable Isotopes ($\delta^{18}\text{O}$, $\delta^2\text{H}$) of Pore Waters in
10 Clay-Rich Aquitards: A Comparison and Evaluation of Measurement Techniques, 108–116,
11 2001.

12 Kendall, C. and McDonnell, J. J.: Isotopes in catchment hydrology, Elsevier, 2012.

13 Koeniger, P., Gaj, M., Beyer, M., and Himmelsbach, T.: Review on soil water stable isotope
14 based groundwater recharge estimations, *Hydrol. Process.*, submitted.

15 Koeniger, P., Marshall, J. D., Link, T., and Mulch, A.: An inexpensive, fast, and reliable
16 method for vacuum extraction of soil and plant water for stable isotope analyses by mass
17 spectrometry, *Rapid Commun. Mass Spectrom.*, 25 (20), 3041–3048, doi:10.1002/rcm.5198,
18 2011.

19 Lindenmaier, F. and Christelis, G. (Eds.): Groundwater for the North of Namibia: Summary
20 Report of Activities of Phase I, Exploration of Ohangwena II Aquifer and Preliminary Isotope
21 Study, Volume 1a, Windhoek, 2012.

22 Lindenmaier, F., Lohe C., and Quinger M.: Groundwater for the North of Namibia: Executive
23 Summary Phase I, Windhoek, 2014.

24 Lee, K.S., Kim, J.M., Lee, D.-R., Kim, Y., and Lee, D.: Analysis of water movement through
25 an unsaturated soil zone in Jeju Island, Korea using stable oxygen and hydrogen isotopes,
26 *Journal of Hydrology*, 345 (3-4), 199–211, doi:10.1016/j.jhydrol.2007.08.006, 2007.

27 Mendelsohn, J., Jarvis A., Robertson T., Mendelsohn, J., Jarvis, A., and Robertson, T.: A
28 Profile and Atlas of the Cuvelai - Etosha Basin, RAISON; Gondwana Collection, Windhoek,
29 Namibia, 172 // 170, 2013.

1 Merlivat L.: Molecular diffusivities of H₂16O, HD₁₆O, and H₂18O in gases, The Journal of
2 chemical Physics (69), doi:10.1063/1.436884, 1978.

3

4 Mueller, M. H., Alaoui, A., Kuells, C., Leistert, H., Meusburger, K., Stumpp, C., Weiler, M.,
5 and Alewell, C.: Tracking water pathways in steep hillslopes by $\delta^{18}\text{O}$ depth profiles of soil
6 water, Journal of Hydrology (519), 340–352, doi:10.1016/j.jhydrol.2014.07.031, 2014.

7 Or, D., Lehmann, P., Shahraeeni, E., & Shokri, N. (2013). Advances in soil evaporation
8 physics—A review. *Vadose Zone Journal*, 12(4).

9 Orlowski, N., Frede, H.-G., Brüggemann, N., and Breuer, L.: Validation and application of a
10 cryogenic vacuum extraction system for soil and plant water extraction for isotope analysis, J.
11 Sens. Sens. Syst. (2), 179–193, doi:10.5194/jsss-2-179-2013, 2013.

12 Rambo, J., Lai C-T., and Farlin J.: On-Site Calibration for High Precision Measurements of
13 Water Vapor Isotope Ratios Using Off-Axis Cavity-Enhanced Absorbtion Spectroscopy,
14 Journal of Atmospheric and Oceanic Technology (28), 1448–1457, 2011.

15 Richard, P. and Shoemaker, C. A.: A Comparison of Chemical and Isotopic Hydrograph
16 Separation, Water Resour. Res. (22(10)), 1444–1454, 1986.

17 Rothfuss, Y., Vereecken, H., and Brüggemann, N.: Monitoring water stable isotopic
18 composition in soils using gas-permeable tubing and infrared laser absorption spectroscopy,
19 Water Resour. Res., 49 (6), 3747–3755, doi:10.1002/wrcr.20311, 2013.

20 Rothfuss, Y., Merz, S., Vanderborght, J., Hermes, N., Weuthen, A., Pohlmeier, A.,
21 Vereecken, H., and Brüggemann, N.: Long-term and high frequency non-destructive
22 monitoring of water stable isotope profiles in an evaporating soil column, Hydrol. Earth Syst.
23 Sci. Discuss., 12, 3893-3918, doi:10.5194/hessd-12-3893-2015, 2015.

24 Saxena, R. K.: Oxygen-18 fractionation in nature and estimation of groundwater recharge,
25 Uppsala University, Department of Physical Geography, Divisidion of Hydrology, 1987.

26 Scanlon, B. R., Healy, R. W., and Cook, P. G.: Choosing appropriate techniques for
27 quantifying groundwater recharge, Hydrogeology Journal, 10 (1), 18–39,
28 doi:10.1007/s10040-001-0176-2, 2002.

29 Schack-Kirchner, H., Hildebrand, E. E., and Wilpert, K. von: Ein konvektionsfreies
30 Sammelsystem für Bodenluft, Pflanzenernährung und Bodenkunde (156), 307–310, 1993.

1 Singleton, M. J., Sonnenthal, E.L, Conrad, M.E., DePaolo, D., and Gee, G. W.: Multiphase
2 Reactive Transport Modeling of Seasonal Infiltration Events and Stable Isotope Fractionation
3 in Unsaturated Zone Pore Water and Vapor at the Hanford Site, Vadose Zone Journal (3),
4 775–785, 2004.

5 Sklash, M. G. and Farvolden, R. N.: The role of groundwater in storm runoff., Journal of
6 Hydrology (43), 45–65, 1979.

7 Soderberg, K., Good, S. P., Wang, L., and Caylor, K.: Stable Isotopes of Water Vapor in the
8 Vadose Zone: A Review of Measurement and Modeling Techniques, Vadose Zone Journal,
9 11 (3), 0, doi:10.2136/vzj2011.0165, 2012.

10 Sutanto, S. J., van den Hurk, B., Dirmeyer, P. A., Seneviratne, S. I., Röckmann, T., Trenberth,
11 K. E., Blyth, E. M., Wenninger, J., and Hoffmann, G.: HESS Opinions "A perspective on
12 isotope versus non-isotope approaches to determine the contribution of transpiration to total
13 evaporation", Hydrol. Earth Syst. Sci., 18 (8), 2815–2827, doi:10.5194/hess-18-2815-2014,
14 2014.

15 Sprenger, M., Volkmann, T. H. M., Blume, T., and Weiler, M.: Estimating flow and transport
16 parameters in the unsaturated zone with pore water stable isotopes, Hydrol. Earth Syst. Sci.
17 Discuss., 11 (10), 11203–11245, doi:10.5194/hessd-11-11203-2014, 2014.

18 Stumpp, C. and Maloszewski, P.: Quantification of preferential flow and flow heterogeneities
19 in an unsaturated soil planted with different crops using the environmental isotope $\delta^{18}\text{O}$,
20 Journal of Hydrology, 394 (3-4), 407–415, doi:10.1016/j.jhydrol.2010.09.014, 2010.

21 Sturm, P. and Knohl, A.: Water vapor $\delta^2\text{H}$ and $\delta^{18}\text{O}$ measurements using off-axis integrated
22 cavity output spectroscopy, Atmos. Meas. Tech., 3 (1), 67–77, doi:10.5194/amt-3-67-2010,
23 2010.

24 Skrzypek, G., Mydłowski, A., Dogramaci, S., Hedley, P., Gibson, J. J., & Grierson, P. F.
25 (2015). Estimation of evaporative loss based on the stable isotope composition of water using
26 Hydrocalculator. *Journal of Hydrology*, 523, 781-789.

27 Tetzlaff, D., Soulsby, C., Waldron, S., Malcolm, I. A., Bacon, P. J., Dunn, S. M., Lilly, A.,
28 and Youngson, A. F.: Conceptualization of runoff processes using a geographical information
29 system and tracers in a nested mesoscale catchment, Hydrol. Process., 21 (10), 1289–1307,
30 doi:10.1002/hyp.6309, 2007.

1 van Geldern, R. and Barth, J. A.: Optimization of instrument setup and post-run corrections
2 for oxygen and hydrogen stable isotope measurements of water by isotope ratio infrared
3 spectroscopy (IRIS), Limnol. Oceangr. Methods (10), 1024–1036,
4 doi:10.4319/lom.2012.10.1024, 2012.

5 Volkmann, T. and Weiler, M.: Continual in-situ monitoring of pore water stable isotopes,
6 Hydrol. Earth Syst. Sci. (18), 1819–1833, doi:10.5194/hess-18-1819-2014, 2013.

7 Walker, G. R., Woods, P. H., and Allison, G. B.: Interlaboratory comparison of methods to
8 determine the stable isotope composition of soil water, Chemical Geology, 111 (1-4), 297–
9 306, doi:10.1016/0009-2541(94)90096-5, 1994.

10 Wang, L., Caylor, K., and Dragoni, D.: On the calibration of continuous, high-precision $d^{18}\text{O}$
11 and $d^2\text{H}$ measurements using an off-axis integrated cavity output spectrometer (23), 530–536,
12 2009.

13 Wang, L., Good, S. P., Caylor, K. K., and Cernusak, L. A.: Direct quantification of leaf
14 transpiration isotopic composition, Agricultural and Forest Meteorology (154-155), 127–135,
15 doi:10.1016/j.agrformet.2011.10.018, 2012.

16 Wassenaar, L. I., Hendry, M. J., Chostner V.L., and Lis G.P.: High Resolution Pore Water ^2H
17 and ^{18}O Measurements by $\text{H}_2\text{O}_{(\text{liquid})}\text{H}_2\text{O}_{(\text{vapor})}$ Equilibration Laser Spectroscopy,
18 Environmental Science and Technology (42), 9262–9267, 2008.

19 West, A. G., Patrickson, S.J., Ehleringer, J.R.: Water extraction times for plant and soil
20 materials used in stable isotope analysis, Rapid Commun. Mass Spectrom. (20): 1317-1321,
21 2006.

22 Western, Andrew W.; Zhou, Sen-Lin; Grayson, Rodger B.; McMahon, Thomas A.; Blöschl,
23 Günter; Wilson, David J. (2004): Spatial correlation of soil moisture in small catchments and
24 its relationship to dominant spatial hydrological processes. *Journal of Hydrology* 286 (1-4), S.
25 113–134. DOI: 10.1016/j.jhydrol.2003.09.014.

26 Wilson G.W., Fredlund D.G., and Barbour S.L.: The effect of soil suction on evaporative
27 fluxes from soil surfaces., Can. Geotech. Journal (34), 145–155, 1997.

28 Wu, Y., Zhou, H., Zheng, X.-J., Li, Y., and Tang, L.-S.: Seasonal changes in the water use
29 strategies of three co-occurring desert shrubs, Hydrol. Process., 28 (26), 6265–6275,
30 doi:10.1002/hyp.10114, 2014.

- 1 Yang Q., Xiao, H., Zhao, L., Zhou, M., and Li, C., Coa, S.: Stable isotope techniques in plant
- 2 water sources: a review, *Science in Cold and Arid Regions* (2), 0112–0122, 2010.
- 3 Zimmermann, U., Münnich K.O., and Roether W.: Downward movement of soil moisture
- 4 traced by means of hydrogen isotopes, *Geophysical Monograph Series* (11), 1967.

1 **Table 1: Standards used for normalization, drift correction, quality check. The standards are used for**
 2 **both, the measurements with the in-situ approach in the field and for the extracted soil water in the**
 3 **laboratory.**

Abbreviation	Description	$\delta^2\text{H}$ [%]	σ	$\delta^{18}\text{O}$ [%]	σ
HMER	Hannover sea water	-3.1 \pm 0.4		-0.4 \pm 0.13	
HDES	Hannover distilled water	-55.9 \pm 0.9		-8.12 \pm 0.14	
HLAU	Hannover lauretaner water	-64.6 \pm 0.6		-9.73 \pm 0.10	
HGLA	Hannover glacier water	-152.1 \pm 0.9		-20.27 \pm 0.11	

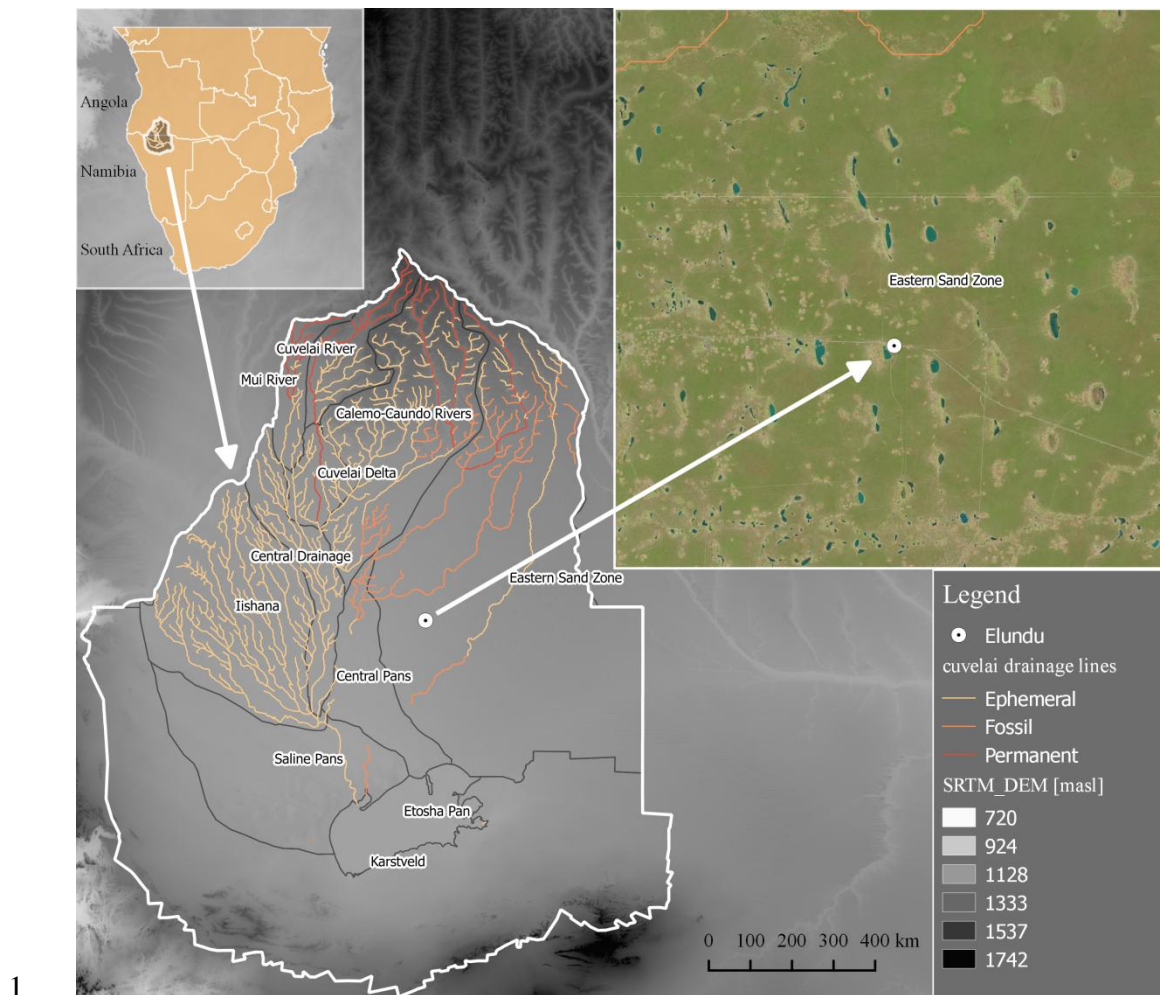
4
 5 **Table 2: Values for HLAU (qc) with the corresponding standard deviation of their repetitive**
 6 **measurements (σ_{qc}), the mean standard deviation of the repetitive measurements of each measurement**
 7 **point (σ_{rep}) and the corresponding values of the cryogenic vacuum extraction (σ_{cry}) from the campaigns**
 8 **June / November 2014. Bare plots (B) and vegetated plots (V) were measured.**

ID	Date	Init.Time	$\delta^2\text{H}_{\text{qc}}$ [%]	σ_{qc}	σ_{rep}	σ_{cry}	$\delta^{18}\text{O}_{\text{qc}}$ [%]	σ_{qc}	σ_{rep}	σ_{cry}	
E1.1	04.06.2014	09:30:00	B	-60.09 \pm 5.13	1.4	3.7	-10.04 \pm 0.66	0.7	0.8		
E1.2	04.06.2014	15:30:00	V	-74.96 \pm 2.83	3	3.5	-13.16 \pm 0.01	0.6	0.6		
			\bar{X}	\pm 3.98	2.2	3.6		\pm 0.34	0.65	0.70	
E2.1	15.11.2014	10:50:00	B	-73.25 \pm 0.87	1.17		-10.38 \pm 0.34	0.45			
E2.2	16.11.2014	08:00:00	B	-69.83 \pm 0.99	1.26		-8.05 \pm 0.48	0.35			
E2.3	16.11.2014	13:30:00	V	-71.11 \pm 0.49	2.21		-10.29 \pm 0.14	0.54			
E2.4	17.11.2014	11:00:00	V	-57.51 \pm 4.11	1.72		-8.45 \pm 0.14	0.28			
E2.5	18.11.2014	11:00:00	V	-64.82 \pm 1.86	1.52		-7.73 \pm 0.34	0.28			
E2.6	19.11.2014	07:30:00	B	-75.62 \pm 1.84	2.49		-6.81 \pm 0.81	0.5			
E2.7	19.11.2014	14:00:00	B	-79.35 \pm 1.27	1.93	3.5	-11.62 \pm 0.36	0.45	0.45		
E2.8	20.11.2014	11:30:00	V	-25.24 \pm 2.53	1.45		-3.68 \pm 0.25	0.24			
E2.9	21.11.2014	11:30:00	V	-23.00 \pm 17.17	1.74		-15.59 \pm 4.17	0.37			
			\bar{X}		2.15	1.86	3.57		0.36	0.46	0.62

1 **Table 3:** Soil evaporation (E) is derived from stable isotope depth profiles. The isotope value of the
 2 reservoir δ_{res} , the evaporating front δ_{ef} and the effective depth z_{ef} are estimated from a exponential fit to
 3 the isotope depth profiles. The Soil water storage (S) is calculated from the soil moisture depth profile.
 4 Transpiration (T) is the remainder from annual precipitation (P=660 mm) after subtracting the Recharge
 5 (R=4 and 5 mm for ^2H and ^{18}O , respectively), E and S. The partitioning between soil evaporation to
 6 transpiration is calculated as the contribution of transpiration (E/T_{pot}) to evapotranspiration = $E+T$.

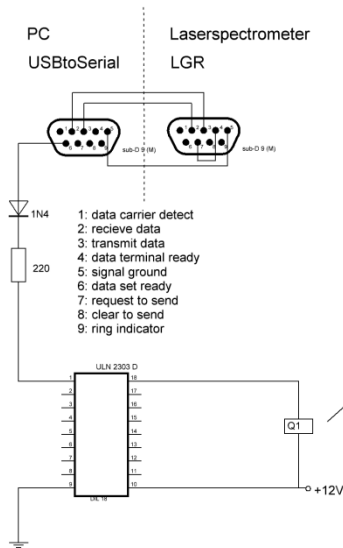
^{18}O

	z_{ef} [mm]	δ_{res} [‰]	δ_{ef} [‰]	E [mm/y]	S [mm]	T [mm/y]	E/T_{pot} [%]
Cryo							
<i>bare</i>	155	-8.2	31.4	147	125	40	468
<i>vegetated</i>	127	-5.2	32.5	179	151	9.5	467
<i>Wet</i>	79	-4.8	5.4	349	295	122	184
In-situ							
<i>bare</i>	115	-6.4	46	197	167	40	418
<i>vegetated</i>	139	-7.4	34.6	164	139	9.5	482
<i>Wet</i>	86	-5.8	5.9	321	271	122	212
^2H							
Cryo							
<i>bare</i>	388	-84.1	21.8	59	49	40	557
<i>vegetated</i>	364	-62.9	8.5	62	53	9.5	585
<i>Wet</i>	90	-26	28.7	307	259	122	227
In-situ							
<i>bare</i>	225	-65	49	101	86	40	515
<i>vegetated</i>	174	-42	69	131	111	9.5	516
<i>Wet</i>	82	-32.8	27	336	285	122	198

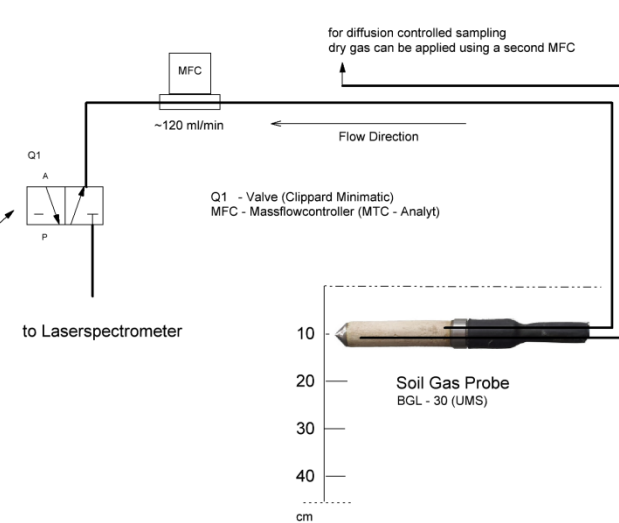


1 **Figure 1: The study area is located in the northern part of the Cuvelai-Etosha-Basin (CEB),**
 2 **which is subdivided by the political border between Angola and Namibia (left). Sampling was**
 3 **conducted in Elundu located in the center of the CEB (center, right).**

Electronic Control

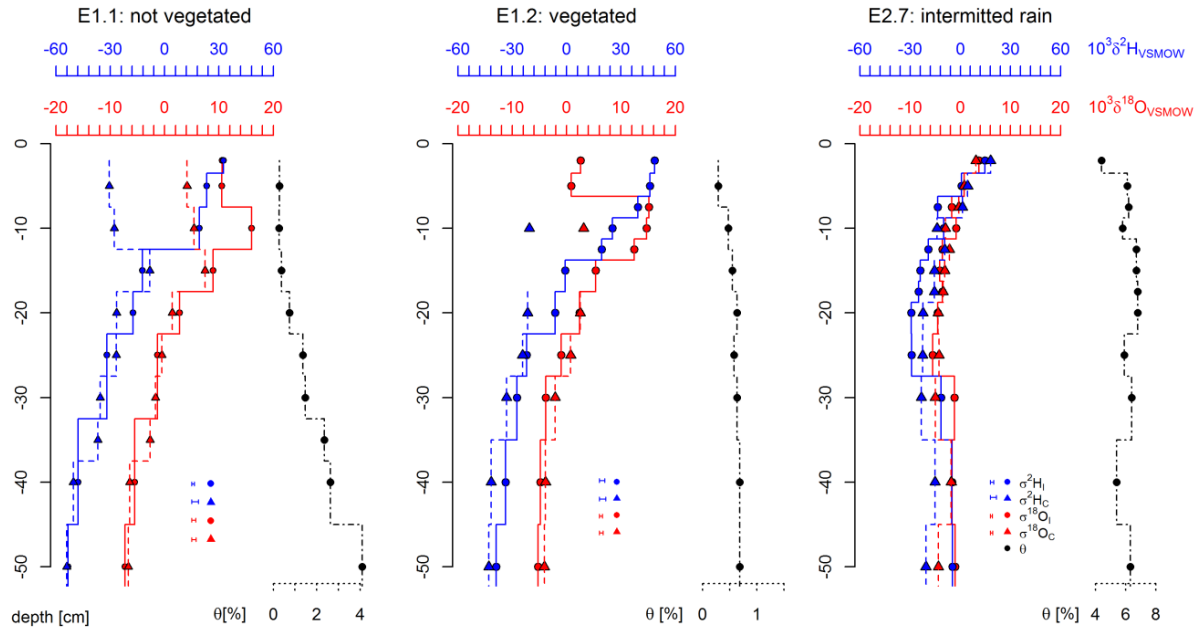


Gas Transport Line



3 **Figure 2: Gas transport (right) is controlled by an automated electronic control (left). The PC**
 4 **mimics the behavior of a laboratory autosampler communicating with the analyser via an USBto**
 5 **Serial adapter. High and low signals from the data set ready pin can be used to switch valves**
 6 **using an optocoupler (ULN2303). Vapor is transported via the transport line from the soil gas**
 7 **probe to the ICOS device. The flow is measured with a mass flow controller (MFC).**

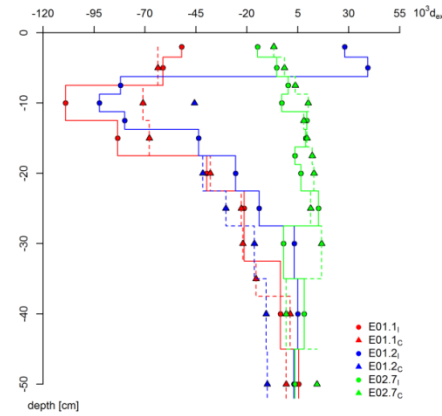
1



2

3 **Figure 3: Depths profiles of the field campaign in June 2014 (E1.1, E1.2) and the field campaign**
4 **in November 2014 (E2.7) are shown. Compared are isotope depth profiles extracted with the**
5 **cryogenic vacuum extraction (dashed, triangles) and measured in-situ (straight, dots). $\delta^2\text{H}$ is**
6 **given in blue and $\delta^{18}\text{O}$ is given in red. Soil moisture is illustrated on the right of each plot**
7 **(black). Standard deviation for each plot and each method is indicated by error bars in the**
8 **legend of the plot.**

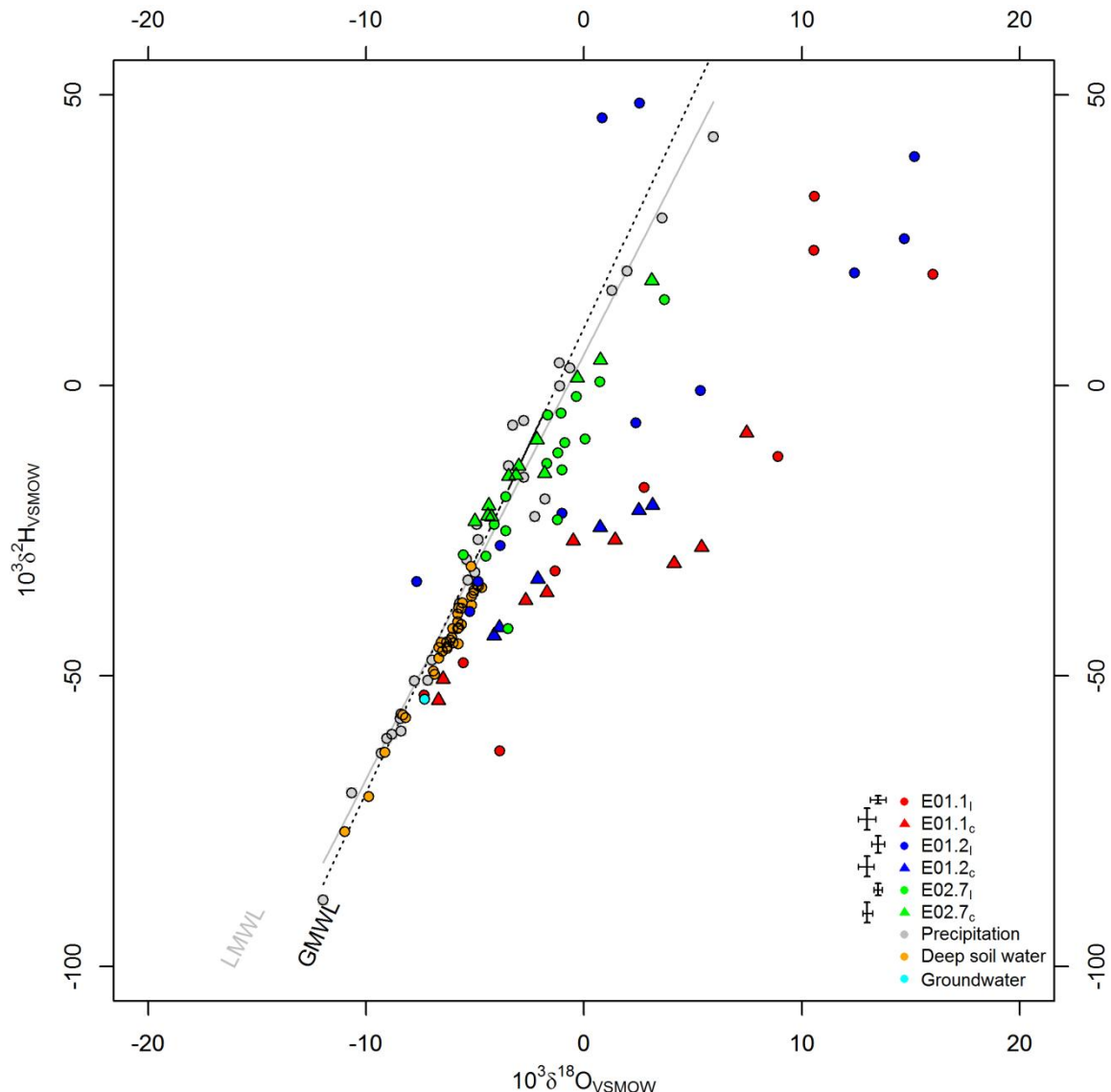
9



10

11 **Figure 4: Deuterium excess for the profiles E01.1, E01.2 sampled in June 2014 and E02.7**
12 **sampled in November 2014. Compared are values from the cryogenic vacuum extraction**
13 **(triangles) and the in-situ measurements (circles).**

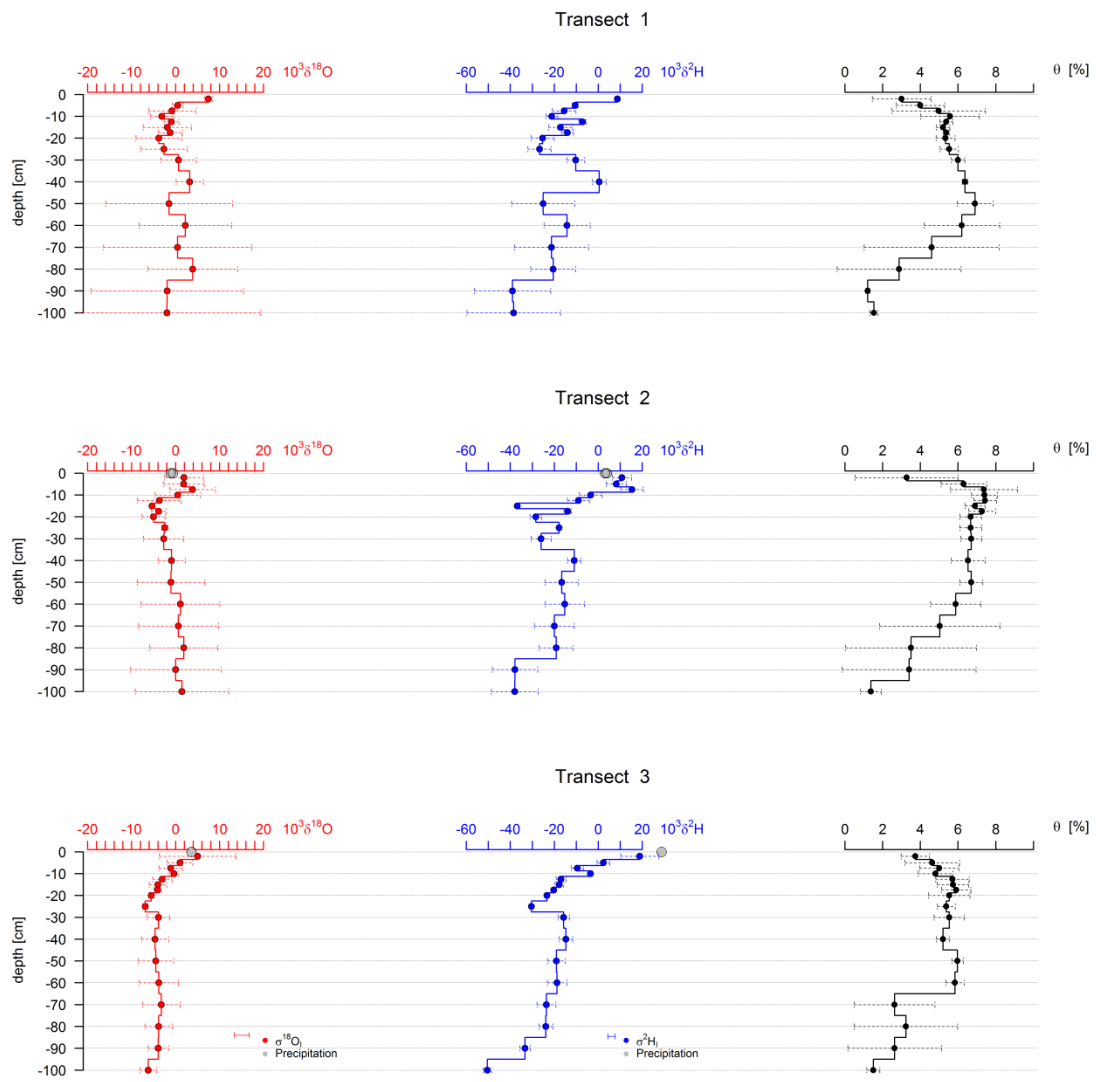
1



2

3 **Figure 5: $\delta^{18}\text{O}$ vs $\delta^2\text{H}$ plot of the profiles E01.1, E01.2, E02.7. Further shown is the local**
 4 **meteoric water line (LMWL) for the northern part of Namibia as well as the global meteoric**
 5 **water line (GMWL). A mean value of shallow groundwater is plotted and additionally soil water**
 6 **of a depth profile down to a depth of 4 m.**

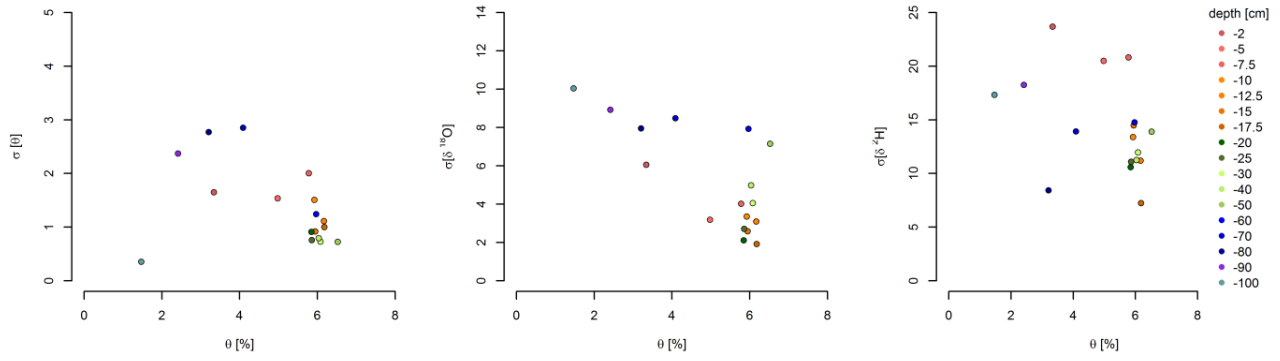
7



1

2 **Figure 6:** ^{18}O (red), ^2H (blue) and soil moisture (black) depth profiles. Shown are mean values
 3 for three transects consisting of three single profiles derived from in-situ measurements. Mean
 4 standard deviation σ of all quality check standards (qc) are shown in the legend. Rainfall isotope
 5 values are indicated on the x-axes in grey.

6



1

2 **Figure 7: Mean soil moisture (Θ) for each depth plotted against the standard deviation of soil**
 3 **moisture $\sigma[\Theta]$ between each depth as well as standard deviation of $\sigma[\delta^{18}\text{O}]$ and $\sigma[\delta^2\text{H}]$,**
 4 **respectively.**

5